

Valley polarization in twisted altermagnetism

San-Dong Guo^{†*}

School of Electronic Engineering, Xi'an University of Posts and Telecommunications, Xi'an 710121, China

Yichen Liu[†] and Cheng-Cheng Liu[‡]

*Centre for Quantum Physics, Key Laboratory of Advanced Optoelectronic Quantum Architecture and Measurement (MOE),
School of Physics, Beijing Institute of Technology, Beijing 100081, China*

The combination of altermagnetism, twistronics and valleytronics is of great significance for potential applications in advanced electronic devices. Twisted magnetic van der Waals bilayers have been identified as an ideal platform for altermagnetism of any type, such as *d*-wave, *g*-wave, and *i*-wave, by choosing the constituent monolayer with specific symmetry [arXiv:2404.17146 (2024)]. Here, we propose a way for achieving valley polarization in twisted altermagnetism by applying out-of-plane external electric field. Since the out-of-plane electric field creates a layer-dependent electrostatic potential, the valleys from different layers will stagger, producing valley polarization. We also demonstrate the effectiveness of our proposed way using the twisted tight-binding model. It is found that the applied electric field can also induce valley/spin-gapless semiconductor and half metal besides valley polarization. Based on first-principles calculations, our proposed way to achieve valley polarization can be verified in twisted bilayer VObR and monolayer Ca(CoN)₂ as a special twisted altermagnet. These findings provide new opportunities for innovative spintronics, twistronics and valleytronics applications.

INTRODUCTION

Due to lacking any net magnetic moment, the antiferromagnetic (AFM) materials are robust to external magnetic perturbation, and have ultra-high dynamic speed[1, 2]. In general, these AFM materials lack spin splitting, which is considered not to be conducive to the generation of spin-polarized currents[3]. Recently, a category of collinear crystal-symmetry compensated magnetic ordering called altermagnetism has been emerging as an exciting research landscape[4–7]. The altermagnetism can realize spin-splitting, which is only originated from the simple AFM ordering of special magnetic space group without the help of relativistic spin-orbital coupling (SOC). Several bulk and two-dimensional (2D) materials have been predicted to be altermagnetism[8–16].

Twisted-angle 2D systems exhibit novel and tunable properties, such as flat bands, nontrivial topology, emergent symmetries, enhanced correlations, and strong electron-phonon coupling, due to the charge localization induced by the formation of moiré superlattice[17–22]. Twisted magnetic systems have also been extensively studied due to their novel properties[23–27], including magnetic ground states, multiflavor magnetic states, non-relativistic spin-momentum coupling, noncollinear magnetic states and moiré magnon bands. Recently, altermagnetism has been achieved in twisted magnetic van der Waals (vdW) bilayers by introducing a key in-plane 2-fold rotational operation, which takes one of all five 2D Bravais lattices[28]. The symmetry of spin splitting, i.e., *d*-wave, *g*-wave or *i*-wave, can be realized by choosing out-of-plane rotational symmetry. Twisted altermagnetism provides a general, adjustable and ideal platform to explore multifunctional features, for example a combi-

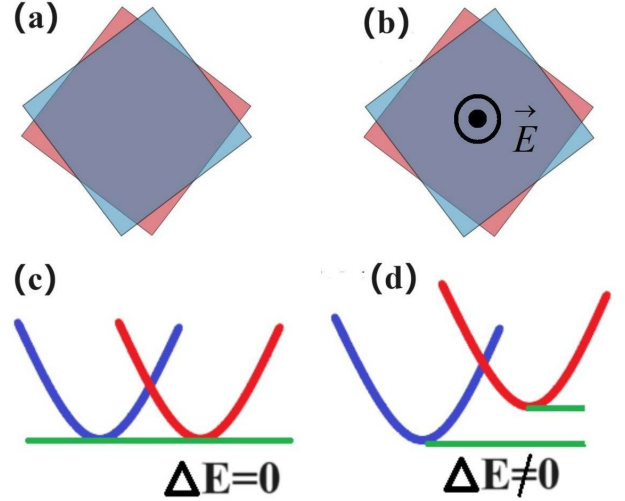


FIG. 1. (Color online)(a)/(b): a twisted altermagnetic bilayer without/with out-of-plane electric field; (c) and (d): two valleys near the Fermi level are from different layers with opposite spin polarization. For (a) case, the degeneracy of electron spin is removed, but it lacks valley polarization (c). For (b) case, the degeneracy of both spin and valley are lifted, producing spin-valley polarization (d). In (b), the black dotted circle means an out-of-plane electric field. In (c) and (d), the spin-up and spin-down channels are depicted in blue and red.

nation of altermagnetism, twistronics and valleytronics.

Valleytronics by utilizing valley degree of freedom to encode and process information provides remarkable opportunities for developing energy-efficient devices [29–32]. In AFM materials especially for altermagnetism, realizing valley polarization is more meaningful for valleytronic application. Twisted altermagnetism provides a general platform for exploring valley polarization, be-

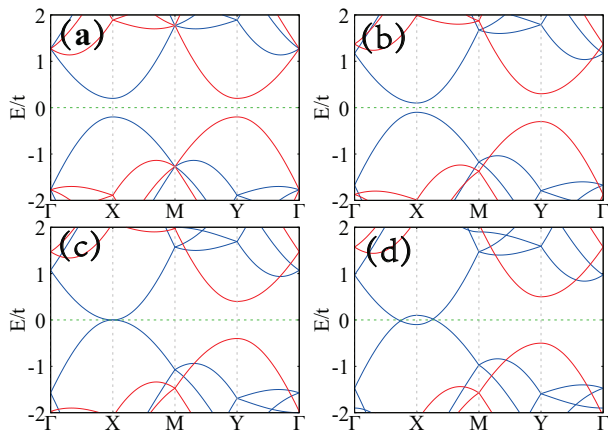


FIG. 2. (Color online) The energy band structure of the twisted model without (a)/with (b, c, d) electric field by using $\delta = 0.0t$ (a), $0.1t$ (b), $0.2t$ (c), $0.3t$ (d). The spin-up and spin-down channels are depicted in blue and red. The other parameters $t_1 = -0.5t_2 = t$, $M = 3.2t$ are chosen.

cause it can possess two equivalent valleys from different layers[28]. Out-of-plane electric field can eliminate the degeneracy of valleys from different layers[33]. Here, we propose a way to achieve valley polarization by electric field in twisted altermagnets.

COMPUTATIONAL DETAIL

Within density functional theory (DFT)[34], the spin-polarized first-principles calculations are carried out by using the standard VASP package[35–37] within the projector augmented-wave (PAW) method. We use generalized gradient approximation of Perdew-Burke-Ernzerhof (PBE-GGA)[38] as the exchange-correlation functional. The kinetic energy cutoff of 500 eV, total energy convergence criterion of 10^{-6} eV, and force convergence criterion of $0.001 \text{ eV} \cdot \text{\AA}^{-1}$ are adopted. To account for electron correlation of V-3d and Co-3d orbitals, a Hubbard correction $U_{eff}=3.0 \text{ eV}$ is employed within the rotationally invariant approach proposed by Dudarev et al[39]. By taking a vacuum of more than 16 \AA , the out-of-plane interaction is neglected. A sufficient Monkhorst-Pack k-point meshes are used to sample the Brillouin zone (BZ) for calculating electronic structures.

APPROACH AND MODEL

By using the in-plane 2-fold rotational operation, stacking a twisted bilayer structure with interlayer AFM ordering can construct altermagnetism[28], because the design principle can produce the compensated collinear magnetic order, and make the sublattices with opposite spins connect by a rotation symmetry. The method is a

general approach, which takes one of all five 2D Bravais lattices, including oblique lattice, rectangular/centered-rectangular lattice, square lattice and hexagonal lattice.

Here, we propose a way to achieve valley polarization in twisted altermagnetism, which is valid for all five 2D Bravais lattices. Next, a square lattice, as an example, is used to illustrate our proposal. A twisted bilayer of square lattice with interlayer AFM ordering is shown in Figure 1 (a), which possesses in-plane 2-fold rotational symmetry. We assume that the altermagnetic twisted bilayer possesses two degenerate valleys with opposite spin from different layers near the Fermi level (Figure 1 (c)). To induce valley polarization, an out-of-plane electric field is applied for the altermagnetic twisted bilayer (Figure 1 (b)). Because an out-of-plane electric field can create a layer-dependent electrostatic potential, and the electronic bands in different layer will stagger[33], which gives rise to the valley polarization (Figure 1 (d)). It is also readily comprehensible that the transformation of valley polarization can be achieved by reversing the direction of electric field.

For a square lattice, the Hamiltonian of monolayer model can be expressed as:

$$h(\mathbf{k}) = t_1 \cos(k_x) + t_2 \cos(k_y) \quad (1)$$

where t_i and \mathbf{k} are hopping parameters and wave vector. Firstly, monolayers are stacked into a bilayer structure. And then, by flipping the upper layer, and rotating the upper and lower layers by $-\frac{\theta}{2}$ and $\frac{\theta}{2}$, a moiré supercell can be constructed. The twisted tight-binding (TB) model can be written as[28]:

$$H = \begin{pmatrix} H_{11} & T \\ T^\dagger & H_{22} \end{pmatrix}, \quad (2)$$

$$H_{11} = C_{2\parallel}^m h(R(-\frac{\theta}{2})\mathbf{k})C_{2\parallel}^m + Ms_z + \delta, \quad (3)$$

$$H_{22} = h(R(\frac{\theta}{2})\mathbf{k}) - Ms_z - \delta. \quad (4)$$

Where $C_{2\parallel}^m$ and R are the flip operation and rotation matrix; T , s_z and M represent the interlayer coupling, the spin on each layer and the magnetic moment; $\delta=Ed/2$ with E/d being effective electric field intensity/interlayer distance. Here, the interlayer coupling can be neglected.

The energy band structures of our twisted TB model are plotted in Figure 2 without/with electric field. Without electric field, d -wave altermagnetism can be observed, and two degenerate valleys with opposite spin from different layers, i.e., spin-layer locking, appear in both conduction and valence bands near the Fermi level (Figure 2 (a)). When an out-of-plane electric field is applied, the valley polarization can be achieved (Figure 2 (b)). When continuously increasing E , the valley/spin-gapless semiconductor (Figure 2 (c)) and half-metal (Figure 2 (d))

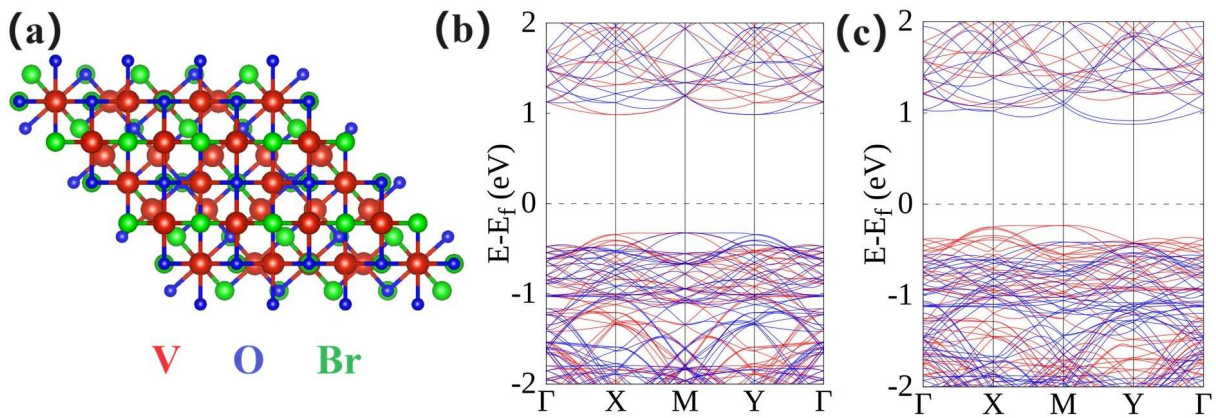


FIG. 3. (Color online) The crystal structures (a) and energy band structure ($E=0$ V/Å (b) and 0.02 V/Å (c)) of twisted bilayer VOBr with the twist angle being 48.16° . The spin-up and spin-down channels are depicted in blue and red.

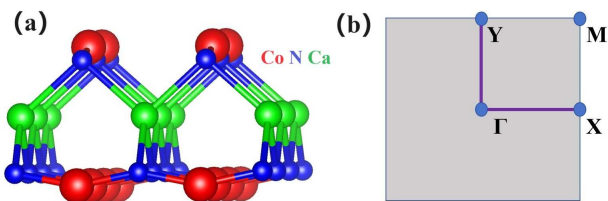


FIG. 4. (Color online) For $\text{Ca}(\text{CoN})_2$ monolayer, the crystal structure (a) and the first BZ with high-symmetry points (b).

can also be realized. For valley/spin gapless semiconductor, both electron and hole can be fully valley/spin polarized[40, 41]. No threshold energy is required to make electrons from occupied states to empty states for these gapless electronic states. The half-metal possesses full electron spin/valley polarization[1]. These electronic states are the most important candidates for applications as spintronic/valleytronic materials.

MATERIAL VERIFICATION

The twisted bilayer VOBr with the twist angle being 48.16° [28] is used as the first example to verify our proposal. The experimental lattice constants $a=3.775$ Å and $b = 3.38$ Å[42] are used to construct twisted bilayer VOBr, and its crystal structures are plotted in Figure 3 (a). Figure 3 (b) and (c) show the intrinsic energy band structure of twisted bilayer VOBr and the one with effective electric field $E=0.02$ V/Å by using GGA+ U with $U=3$ eV. The intrinsic band structures show d -wave altermagnetism, and there are two equivalent valleys with opposite spin from different layers for the conduction bands. When applying an out-of-plane electric field of $E= 0.02$ V/Å, an induced layer-dependent electrostatic potential gives rising to obvious valley splitting for conduction bands, producing spin/valley polarization.

In fact, $\text{Ca}(\text{CoN})_2$ monolayer can be considered as

a special altermagnetic twisted bilayer, and its crystal structure and first BZ are plotted in Figure 4. Monolayer $\text{Ca}(\text{CoN})_2$ has a square lattice structure, whose unit cell contains five atoms with five-atomic layer sequence of Co-N-Ca-N-Co. The $\text{Ca}(\text{CoN})_2$ has been predicted to be an altermagnet with A-type AFM ordering, which is dynamically and thermodynamically stable[43]. The optimized lattice constants $a=b=3.548$ Å by GGA+ U with $U=3$ eV.

Next, we explain why $\text{Ca}(\text{CoN})_2$ monolayer is a special altermagnetic twisted bilayer. The CoN layer can be used as a building block (Figure 5 (a)). Initially, two monolayer CoN are stacked into a bilayer structure that requires AFM ordering (Figure 5 (b)). Subsequently, the lower layer CoN is flipped to introduce an in-plane 2-fold rotational symmetry ((Figure 5 (c))). Then, the upper and lower layers are rotated by 45° and -45° , and the two layers are connected by Ca layer ((Figure 5 (d))). After the twist, the in-plane 2-fold rotational symmetry still remains, which connects two layers with opposite spins and plays a key role in generating altermagnetism. The build process of $\text{Ca}(\text{CoN})_2$ is in accordance with the approach of generating altermagnetism by twisting magnetic vdW bilayers[28].

Figure 5 (e) and (f) show the the energy band structures of $\text{Ca}(\text{CoN})_2$ with $E=0$ V/Å and 0.04 V/Å by using GGA+ U . At $E=0$ V/Å, there are two equivalent valleys for both the conduction and valence bands, and they possess opposite spin from different layers, which provides possibility to induce valley polarization by an out-of-plane electric field. Due to D_2 point group of $\text{Ca}(\text{CoN})_2$, it belongs to d -wave altermagnetism[28]. The total magnetic moment of $\text{Ca}(\text{CoN})_2$ is strictly equal to $0 \mu_B$, and the magnetic moments of two Co atoms are $2.521 \mu_B$ and $-2.521 \mu_B$, respectively. When an out-of-plane electric field of $E= 0.04$ V/Å is applied, a layer-dependent electrostatic potential is induced, give rising to valley splitting of $125/21$ meV for conduction/valence

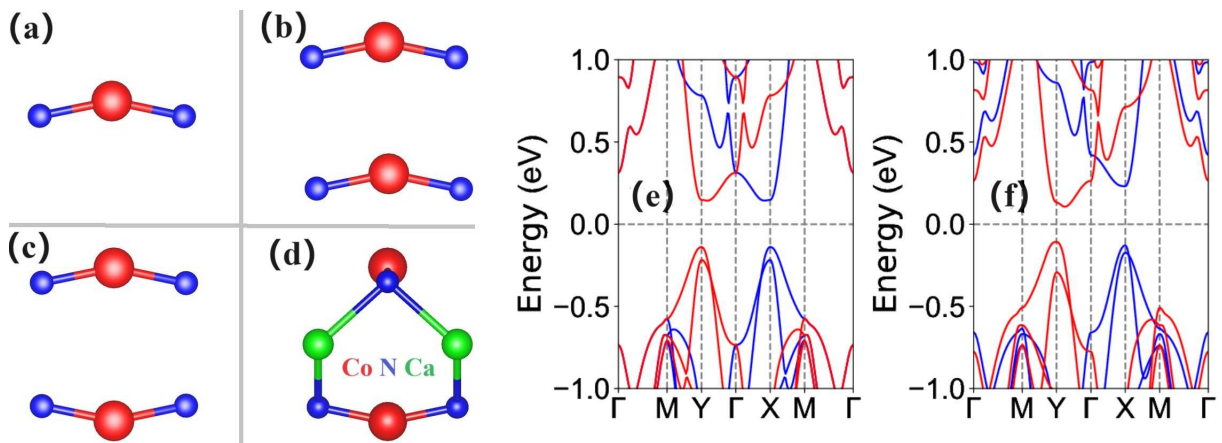


FIG. 5. (Color online)(a): the building block CoN layer; (b): a bilayer structure $(\text{CoN})_2$; (c): the lower layer of $(\text{CoN})_2$ is flipped; (d): a 90° twist operation, and the two layers are connected by Ca layer; (e) and (f): the energy band structures of $\text{Ca}(\text{CoN})_2$ with $E=0 \text{ V/\AA}$ (e) and 0.04 V/\AA (f), and the spin-up and spin-down channels are depicted in blue and red.

bands. In addition, the magnitude of magnetic moments of two Co atoms ($2.508 \mu_B$ and $-2.528 \mu_B$) becomes unequal, although the total magnetic moment of $\text{Ca}(\text{CoN})_2$ is zero.

CONCLUSION

In summary, we propose an alternative strategy to achieve valley polarization based on twisted altermagnetism by applying an out-of-plane electric field. Our proposed way is applicable to all five 2D Bravais lattices, and the key is that twisted altermagnetism has two equivalent valleys from different layers near the Fermi level. This ensures that the external electric field causes the two valleys to experience different potential energies, resulting in valley polarization. It is demonstrated that twisted bilayer VObR and monolayer $\text{Ca}(\text{CoN})_2$ as a special twisted altermagnet are possible candidates for realizing valley polarization. Our works reveal a new 2D family of AFM valleyelectronic materials, which allow multifunctional device applications.

The work is supported by the NSF of China (Grant No. 12374055), the National Key R&D Program of China (Grant No. 2020YFA0308800), and the Science Fund for Creative Research Groups of NSFC (Grant No. 12321004). We are grateful to Shanxi Supercomputing Center of China, and the calculations were performed on TianHe-2.

* sandongyuwang@163.com

† These authors contributed equally to this work.

‡ ccliu@bit.edu.cn

[1] X. Hu, Half-metallic antiferromagnet as a prospective material for spintronics, *Adv. Mater.* **24**, 294 (2012).

- [2] T. Jungwirth, J. Sinova, A. Manchon, X. Marti, J. Wunderlich and C. Felser, The multiple directions of antiferromagnetic spintronics, *Nat. Phys.* **14**, 200 (2018).
- [3] J. Železný, Y. Zhang, C. Felser and B. Yan, Spin-polarized current in noncollinear antiferromagnets, *Phys. Rev. Lett.* **119**, 187204 (2017).
- [4] L. Šmejkal, J. Sinova and T. Jungwirth, Beyond conventional ferromagnetism and antiferromagnetism: A phase with nonrelativistic spin and crystal rotation symmetry, *Phys. Rev. X* **12**, 031042 (2022).
- [5] I. Mazin, Altermagnetisma new punch line of fundamental magnetism, *Phys. Rev. X* **12**, 040002 (2022).
- [6] L. Šmejkal, J. Sinova and T. Jungwirth, Emerging research landscape of altermagnetism, *Phys. Rev. X* **12**, 040501 (2022).
- [7] H.-Y. Ma, M. L. Hu, N. N. Li, J. P. Liu, W. Yao, J. F. Jia and J. W. Liu, Multifunctional antiferromagnetic materials with giant piezomagnetism and noncollinear spin current, *Nat. Commun.* **12**, 2846 (2021).
- [8] L. Šmejkal, R. González-Hernández, T. Jungwirth and J. Sinova, Crystal time-reversal symmetry breaking and spontaneous Hall effect in collinear antiferromagnets, *Sci. Adv.* **6**, eaaz8809 (2020).
- [9] S. López-Moreno, A. H. Romero, J. Mejía-López, A. Muñoz and Igor V. Roshchin, First-principles study of electronic, vibrational, elastic, and magnetic properties of FeF_2 as a function of pressure, *Phys. Rev. B* **85**, 134110 (2012).
- [10] I. I. Mazin, Altermagnetism in MnTe: Origin, predicted manifestations, and routes to detwinning, *Phys. Rev. B* **107**, L100418 (2023).
- [11] M. Naka, S. Hayami, H. Kusunose, Y. Yanagi, Y. Motome and H. Seo, Spin current generation in organic antiferromagnets, *Nat. Commun.* **10**, 4305 (2019).
- [12] L.-D. Yuan, Z. Wang, J.-W. Luo, E. I. Rashba and A. Zunger, Giant momentum-dependent spin splitting in centrosymmetric low-Z antiferromagnets, *Phys. Rev. B* **102**, 014422 (2020).
- [13] M. Naka, Y. Motome and H. Seo, Perovskite as a spin current generator, *Phys. Rev. B* **103**, 125114 (2021).

- [14] S.-D. Guo, X.-S. Guo, K. Cheng, K. Wang, and Y. S. Ang, Piezoelectric altermagnetism and spin-valley polarization in Janus monolayer Cr_2SO , *Appl. Phys. Lett.* **123**, 082401 (2023).
- [15] X. Chen, D. Wang, L. Y. Li and B. Sanyal, Giant spin-splitting and tunable spin-momentum locked transport in room temperature collinear antiferromagnetic semimetallic CrO monolayer, *Appl. Phys. Lett.* **123**, 022402 (2023).
- [16] P. J. Guo, Z. X. Liu and Z. Y. Lu, Quantum anomalous hall effect in collinear antiferromagnetism, *npj Comput. Mater.* **9**, 70 (2023).
- [17] Y. Cao, V. Fatemi, A. Demir, S. Fang, S. L. Tomarken, J. Y. Luo, J. D. Sanchez-Yamagishi, K. Watanabe, T. Taniguchi, E. Kaxiras, R. C. Ashoori and P. Jarillo-Herrero, Correlated insulator behaviour at half-filling in magic-angle graphene superlattices, *Nature (London)* **556**, 80 (2018).
- [18] R. Bistritzer and A. H. MacDonald, moiré bands in twisted double-layer graphene, *Proc. Natl. Acad. Sci. USA* **108**, 12233 (2011).
- [19] S. Carr, D. Massatt, S. Fang, P. Cazeaux, M. Luskin and E. Kaxiras, Twistrionics: Manipulating the electronic properties of two-dimensional layered structures through their twist angle, *Phys. Rev. B* **95**, 075420 (2017).
- [20] M. Angeli, D. Mandelli, A. Valli, A. Amaricci, M. Capone, E. Tosatti and M. Fabrizio, Emergent D_6 symmetry in fully relaxed magic-angle twisted bilayer graphene, *Phys. Rev. B* **98**, 235137 (2018).
- [21] H. C. Po, L. Zou, A. Vishwanath and T. Senthil, Origin of Mott insulating behavior and superconductivity in twisted bilayer graphene, *Phys. Rev. X* **8**, 031089 (2018).
- [22] B. Lian, Z. Wang and B. A. Bernevig, Twisted bilayer graphene: a phonon-driven superconductor, *Phys. Rev. Lett.* **122**, 257002 (2019).
- [23] Y. Xu, A. Ray, Y.-T. Shao, S. Jiang, K. Lee, D. Weber, J. Goldberger, K. Watanabe, T. Taniguchi, D. Muller, K. Mak and J. Shan, Coexisting ferromagnetic/antiferromagnetic state in twisted bilayer CrI_3 , *Nat. Nanotechnol.* **17**, 143 (2022).
- [24] K. Hejazi, Z.-X. Luo and L. Balents, Noncollinear phases in moiré magnets, *Proc. Natl. Acad. Sci. U.S.A.* **117**, 10721 (2020).
- [25] F. Xiao, K. Chen and Q. Tong, Magnetization textures in twisted bilayer CrX_3 ($X=\text{Br}, \text{I}$), *Phys. Rev. Res.* **3**, 013027 (2021).
- [26] C. Wang, Y. Gao, H. Lv, X. Xu and D. Xiao, Stacking domain wall magnons in twisted van der Waals magnets, *Phys. Rev. Lett.* **125**, 247201 (2020).
- [27] R. He, D. Wang, N. Luo, J. Zeng, K. Q. Chen and L. M. Tang, Nonrelativistic spin-momentum coupling in antiferromagnetic twisted bilayers, *Phys. Rev. Lett.* **130**, 046401 (2023).
- [28] Y. Liu, J. Yu and C. C. Liu, Twisted Magnetic Van der Waals Bilayers: An Ideal Platform for Altermagnetism, *arXiv:2404.17146* (2024).
- [29] J. R. Schaibley, H. Yu, G. Clark, P. Rivera, J. S. Ross, K. L. Seyler, W. Yao and X. Xu, Valleytronics in 2D materials, *Nat. Rev. Mater.* **1**, 16055 (2016).
- [30] G. Pacchioni, Valleytronics with a twist, *Nat. Rev. Mater.* **5**, 480 (2020).
- [31] S. A. Vitale, D. Nezich, J. O. Varghese, P. Kim, N. Gedik, P. Jarillo-Herrero, D. Xiao and M. Rothschild, Valleytronics: opportunities, challenges, and paths forward, *Small* **14**, 1801483 (2018).
- [32] D. Xiao, M. C. Chang and Q. Niu, Berry phase effects on electronic properties, *Rev. Mod. Phys.* **82**, 1959 (2010).
- [33] S. D. Guo and Y. S. Ang, Spontaneous spin splitting in electric potential difference antiferromagnetism, *Phys. Rev. B* **108**, L180403 (2023).
- [34] P. Hohenberg and W. Kohn, Inhomogeneous Electron Gas, *Phys. Rev.* **136**, B864 (1964); W. Kohn and L. J. Sham, Self-Consistent Equations Including Exchange and Correlation Effects, *Phys. Rev.* **140**, A1133 (1965).
- [35] G. Kresse, Ab initio molecular dynamics for liquid metals, *J. Non-Cryst. Solids* **193**, 222 (1995).
- [36] G. Kresse and J. Furthmüller, Efficiency of ab-initio total energy calculations for metals and semiconductors using a plane-wave basis set, *Comput. Mater. Sci.* **6**, 15 (1996).
- [37] G. Kresse and D. Joubert, From ultrasoft pseudopotentials to the projector augmented-wave method, *Phys. Rev. B* **59**, 1758 (1999).
- [38] J. P. Perdew, K. Burke and M. Ernzerhof, Generalized gradient approximation made simple, *Phys. Rev. Lett.* **77**, 3865 (1996).
- [39] S. L. Dudarev, G. A. Botton, S. Y. Savrasov, C. J. Humphreys, and A. P. Sutton, Electron-energy-loss spectra and the structural stability of nickel oxide: An LSDA+ U study, *Phys. Rev. B* **57**, 1505 (1998).
- [40] X. L. Wang, Proposal for a new class of materials: spin gapless semiconductors, *Phys. Rev. Lett.* **100**, 156404 (2008).
- [41] S. D. Guo, Y. L. Tao, G. Wang, S. Chen, D. Huang and Y. S. Ang, Proposal for valleytronic materials: Ferrovalley metal and valley gapless semiconductor, *Front. Phys.* **19**, 23302 (2024).
- [42] N. Miao, B. Xu, L. Zhu, J. Zhou and Z. Sun, 2D intrinsic ferromagnets from van der Waals antiferromagnets, *J. Am. Chem. Soc.* **140**, 2417 (2018).
- [43] R. W. Zhang, C. X. Cui, R. Z. Li, J. Y. Duan, L. Li, Z. M. Yu and Y. G. Yao, Predictable gate-field control of spin in altermagnets with spin-layer coupling, *arXiv:2306.08902* (2023).